# Single-Antenna AoA Estimation with UWB Radios

Nour Smaoui
University of Houston
nour@cs.uh.edu

Milad Heydariaan
University of Houston
milad@cs.uh.edu

Omprakash Gnawali
University of Houston
gnawali@cs.uh.edu

*Abstract*—Ultra-wideband (UWB) is becoming a major localization technology enabler for the indoor environment. Traditional localization systems rely on time-of-arrival (ToA)-based methods such as two-way ranging (TWR) and time difference of arrival (TDoA). Such solutions cannot scale due to interference from multiple devices sharing the same part of the wireless spectrum. One solution is to use concurrent transmissions for a more efficient use of air time. Concurrency-based localization systems that utilize ToA cannot satisfy the accuracy requirements of many applications due to hardware time scheduling limitations. Angle of Arrival (AoA) is a promising solution that can provide scalability and accuracy when used in a concurrent transmission scheme. UWB radio platforms like Decawave DWM1002 with dual-UWB-chip design have made it possible to accurately measure AoA by calculating the phase difference of arrival (PDoA). State-of-the-art AoA estimation has then been extended to build self-localization systems with an unlimited number of tags and to handle multiple sources at the same time. These methods require tags with dual-chip design which adds cost and complexity. In this paper, we investigate the idea of estimating AoA on single-chip (single-antenna) tags receiving concurrent UWB signals from dual-chip anchors (intra-anchor concurrency). As opposed to inter-anchor concurrency, intra-anchor concurrency consists of receiving two concurrent packets from two different chips of the same anchor. By estimating AoA on single-chip tags, we reduce the design complexity and the cost of tags by at least 50%. Our results suggest that the single-antenna AoA can achieve performance similar to dual-antenna AoA estimation.

*Index Terms*—UWB, AoA, concurrency

## I. INTRODUCTION

Localization in indoor environments has become a topic of interest to the research community in the past few years as a major application of the Internet of Things (IoT). With GPS being the most commonly used technology in outdoor environments, it performs weakly in indoor environments due to obstructions creating the non-line-of-sight (NLoS) problem especially in small-scale buildings. Many wireless technologies have tackled this problem including WiFi, BLE, RFID, etc. However, ultra-wideband (UWB) radios have been one of the most promising localization technologies due to their high precision and accuracy. A multitude of localization approaches was applied to UWB to satisfy the needs of many applications. In particular, Angle of Arrival (AoA) estimation, a phase-based localization approach, was very promising and showed more benefits compared to time-based approaches like two-way ranging (TWR) and time difference of arrival (TDoA) [1]. However, AoA solutions usually require the receiver to have an array of antennas since AoA is based on the calculation of the phase difference of a single signal received at two different antennas, which increases the hardware and software design complexities and cost.

The main issues preventing UWB AoA-based systems to become more practical are the system design complexity and the total manufacturing cost due to the requirement of using an array of antennas. The cost overhead significantly affects large-scale self-localization systems. As UWB is starting to be integrated into the car and mobile industries, the scale of the applications is expected to rise further. Hence, reducing the number of chips per receiver from two to one would be crucial in large-scale systems.

Ideally, one UWB radio should be able to switch between an array of antennas to be able to estimate AoA by calculating PDoA of a received signal. To the best of our knowledge, such UWB radios are not commercially available. Another option is to use a dual-chip design with a tight clock synchronization which makes the design and implementation of AoA-based systems very challenging and costly. Additionally, AoA-based localization systems have to deal with front-back ambiguity problem [1]. AoA-based localization solutions can have two architectures:

- **Single-antenna tags and dual-antenna anchors**: In this architecture, the tag sends a packet to the anchor that would be received on both UWB chips and calculates the angle. This solution is not scalable in the presence of a large number of tags as they need to send their packets at different time slots to avoid packet collisions. Decawave DWM1002 [2] platform combines AoA along with TWR to provide a single-anchor localization system, but it does not address the tag scalability problem.

- **Dual-antenna tag and single-antenna anchor**: In this architecture, the anchor sends a packet and the tag receives on both UWB chips and calculates the angle. This solution is scalable as the number of transmitting anchors can be small and can be scheduled in different time slots. With the usage of inter-anchor concurrency, solutions like AnguLoc [1] managed to make it more efficient. However, this architecture is not cost-effective as described earlier.

In this work, we explore a different approach of estimating the AoA that reduces the cost and design complexity. We adapt a single-antenna tag and dual-antenna anchor. However, to avoid the scalability issue, we invert the role of transmitters making the anchors send packets from their dual antennas and the tag receives the packets and calculates the AoA.

We consider two separate cases: (1) The dual-antenna anchor sends packets with a large delay to allow the tag to receive them as two separate packets; (2) The anchor schedules packet transmissions with a delay sufficiently small to send the packets concurrently from its chips and for the tag to receive both packets combined as a single packet. This is where we introduced the notion of intra-anchor concurrency, in contrast with the inter-anchor concurrency where different anchors send their packets concurrently. In intra-anchor concurrency, the chips within the same anchor send their packets concurrently. In the case of separate transmissions, the phases of the first and second packets are the first path phases collected from the Channel Impulse Response (CIR) of each packet. As for the intra-anchor concurrency, the phases of the first and second packets are extracted from the same CIR of the received combined packet, where the phase of the first packet is the phase of the first path. While the phase of the second path is the phase of the second peak in the same CIR.

We implement and evaluate our system on Decawave platform. Our results suggest that the single antenna AoA approach can achieve performance similar to the dual antenna approach.

In this paper, we make these contributions:

- We present the first study of the feasibility of AoA estimation on single-antenna UWB radios and comparison with dual-antenna AoA estimation baseline.
- Study the impact of different transmission delays from dual-antenna UWB radios on the performance of single-antenna AoA estimation and explore the necessity of intra-anchor concurrency.
- Implementation and evaluation of Single antenna AoA on a Decawave hardware platform to understand the real-world feasibility.

## II. RELATED WORK

In this paper, we study AoA estimation on a single-antenna system combined with intra-anchor concurrency. The purpose is to provide a scalable and cost-efficient solution. In this section, we present the mainly related topics to this work as follows.

### A. Wireless Interference Exploitation

Wireless interference was usually regarded as a major source of unreliability in wireless communications. Over the years, multiple solutions aimed to either avoid or mitigate the interference. Examples of interference avoidance techniques are TDMA, random access/back-off methods, and traffic reduction [3]. Examples of interference mitigation techniques are FEC correction, non-linear filters [4], and matched filters [5].

However, interference can be beneficial in many applications. Glossy [6] managed to create a time synchronization scheme through constructive interference while keeping 99.99% reliability. Splash [7] exploited the same idea of Glossy and combined it with channel switching to increase further the data dissemination in the network. SurePoint [8]

also used similar methods to floor time synchronization information in the network while increasing packet reliability. A recent work [9] made use of Glossy to demonstrate the use of concurrent transmissions to increase the reliability in multi-hop UWB networks.

In recent work, TX concurrency was used in UWB in a different way where the concurrency purpose switched from improving packet reliability to providing a concurrent and efficient localization system. It was initially presented by Corbalan and Picco in the context of Single-Sided Two-Way Ranging (SS-TWR) [10] where response messages are sent concurrently. And later elaborated in further studies [11–14]. In all these works, the main issue is related to hardware timing uncertainties and the proposed solutions require multiple rounds of ranging to reduce the timing errors.

### B. Concurrent AoA estimation with UWB radios

In later work, concurrent AoA estimation based-localization was employed. In the case of AoA estimation, the localization system relies on phase estimation which is independent of TX timing uncertainties. In Anguloc [1], a dual-antenna tag and single antenna anchor architecture was adopted. The anchors send concurrently packets to the tags. By applying a peak detection algorithm on the CIR of each chip, phase information is extracted for each anchor. Then an angle estimation for each anchor is calculated. An Angle Difference of Arrival (ADoA) algorithm was applied later to identify the location of each tag. Although this method presents better results than other state-of-the-art methods, it does require the tags to have dual antennas. Wang et al. [15] also exploited the idea of AoA estimation combined with concurrency to improve the single anchor localization proposed by Decawave [16]. However, their solution is not scalable as the CIR information can only accommodate a limited number of tags. Recently a patent by Decawave [17] has proposed the idea of AoA estimation (angle of departure in their context) using a single radio which is equipped with two CIR accumulators.

Our proposed method combines the benefits of using AoA with intra-anchor concurrent transmissions to achieve higher accuracy compared to time-based methods and to reduce the cost and design complexity of AoA localization systems by using single-antenna tags.

## III. SYSTEM DESIGN

Our work is the first system that demonstrates AoA estimation on a single-antenna system. It also studies the impact of transmission delays on AoA estimation.

### A. Dual-antenna AoA estimation

We first describe the background of UWB AoA estimation and how to exploit state-of-the-art techniques in our design. The idea of UWB AoA estimation was first introduced in Decawave's patent [16]. It follows a single-antenna transmitter and a dual-antenna receiver. Figure 1 illustrates the process of path difference calculation that will be used to estimate the AoA. A single-antenna transmitter sends a packet to the
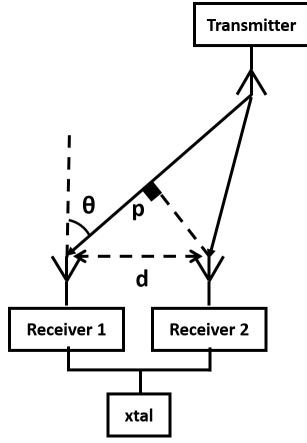
**Fig. 1:** Illustration of classical AoA system. Both receivers are connected to the same clock. The arriving signal angle $\theta$ causes is received on the receiver with path difference p changing therefore the phase of arrival of the signals

dual-antenna receiver. The distance between the antennas is d = 2.08 cm. This distance d is chosen to be less than half the wavelength of the signal $\lambda$ as explained in Decawave patent [18]. This antenna separation d makes both receivers receive the signal with a path difference $p$ ranging from 0 to d. Based on the path difference $p$ we can calculate the angle as $\theta = arcsin(\frac{p}{d})$. As we receive the signal with a path difference $p > 0$, the phases of arrival (PoA) of the signal on both receivers are different. The PoA on each receiver is calculated based on CIR. When the preamble of the packet is received, the UWB chip generates the CIR and detects the first path index. We can compute therefore the phase at the first path index as $PoA = arctan(\frac{Q_i}{I_i})$ with $Q_i$ (respectively $I_i$) being the imaginary (respectively real) part of CIR at the first path index. As both receivers are using the same clock, we can calculate the Phase Difference of Arrival (PDoA), that we denote, $\alpha$ as the difference between the phase of the first receiver and the phase of the second receiver ranging from $-\pi$ to $\pi$ and map it to path difference using the formula $p = \frac{\alpha \times \lambda}{2\pi}$. Path estimation errors can occur due to the antennas asymmetry and therefore require a calibration. More details can be found in both [16] and [1].

### B. Single-antenna AoA estimation

The idea of AoA estimation revolves around estimating the path difference $p$ of the signals between a single-antenna device and two receivers on a dual-antenna device. To be able to perform this phase difference calculation on the single-antenna device, the roles of the transmitter and receiver need to be reversed. Our hypothesis suggests that if two transmitters running on the same clock send two packets separated by a delay $\delta$, the phase difference of the packets on the receiver side should reflect the path difference.

Let's assume that we have two clocks running at the same frequency. At t = 0, the first clock has a phase $P1_0$ and the

second clock has a phase of $P2_0$. Let $\phi_0$ be the phase shift between the first and the second clock at t= 0. After a delay $\delta$, the phase of the first clock $P1_\delta$ and the phase of the second clock $P2_\delta$ will have a phase shift of $\phi_\delta = \phi_0$. Let's denote $PoD_1$ (respectively $PoD_2$) the phase of departure of the first UWB packet from the first chip (respectively the second UWB packet from the second chip). Equation 1 show the difference between both phases of departures with $\Phi$ being the phase shift resulting from the delay within the transmitter clock

$$PoD_2 - PoD_1 = P1_\delta - P1_0 = \Delta_\phi \qquad (1)$$

When both signals arrive at the level of the antenna of the receiver, they arrive with phases of arrival $PoA_1$ (respectively $PoA_2$) defined by equation 2 where $\Phi_{p1}$ (respectively $\Phi_{p2}$) is the phase shift resulting from the signal propagation for a path $p1$ (respectively $p2$). When both signals are processed by the receiver, the term $\Delta_\phi$ will be omitted since the receiver carrier phase will change by $\Delta_\phi$. Therefore the received phase difference is $\Phi_{p2} - \Phi_{p1}$ which is the phase difference resulting from two signals taking two different paths.

$$
\begin{aligned}
PoA_1 &= PoD_1 + \Phi_{p1} \\
PoA_2 &= PoD_2 + \Phi_{p2} \\
PoA_2 - PoA_1 &= PoD_2 - PoD2 + \Phi_{p2} - \Phi_{p1} \\
PoA_2 - PoA_1 &= \Delta_\phi + \Phi_{p2} - \Phi_{p1}
\end{aligned}
\qquad (2)
$$

### 1) Packet transmission scheduling:

As opposed to the classical AoA estimation where a single packet is sent from a single-antenna transmitter, in our design, we have two transmitters on the same device (Figure 3) sending packets sequentially separated by a delay $\delta$ as Figure 2 shows. Based on the value of this delay, there are two possible cases:

**Non-concurrent packet reception**: In this case, the delay is large enough (larger than packet air-time) that the received packets will be detected as two separate packets. In this case, the delay should be at least 188 $\mu$s (time to transmit the full packet) plus the packet processing time before being able to receive the next packet. Since the packets will be received separately, we can identify their phases from the first path of the preamble of each packet.

**Concurrent packet reception**: If the delay is small (smaller than packet preamble transmission time), the transmitted packets will be sent concurrently which refers us to the state-of-the-art work done with inter-node concurrency. In this case, there are two considerations. First, as the path difference p ranges between 0 and 2.08 cm which translates to a few picoseconds. If the packets were to be sent simultaneously, the peaks for the first and second packet will overlap since the CIR granularity is only 1 ns. Second, the system clock used for TX scheduling on DW1000 has a frequency of 124.8 MHz which translates to ~8 ns. Therefore, our delay needs to be a multiple of 8 ns to have accurate TX timestamps.
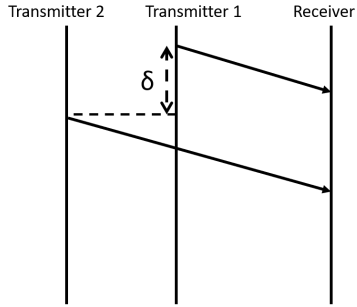
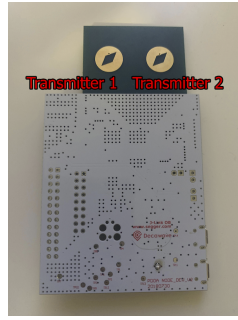**Fig. 2:** Illustration of packet transmission scheduling



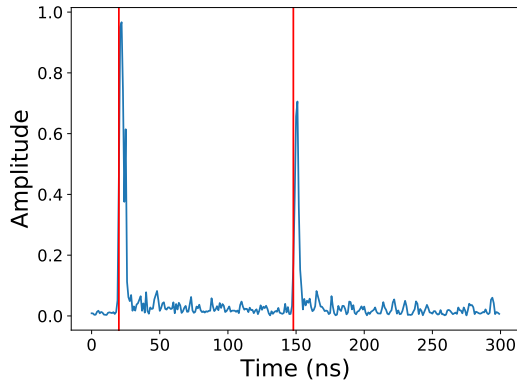**Fig. 3:** Front view of dual-antenna UWB node (DWM1002)



**Fig. 4:** CIR of received concurrent packets delayed by 128 ns shows a first peak at 20 ns and a second peak at around 148 ns

### 2) Peak detection and phase calculation:

In the case of non-concurrent packet reception, the phase of arrival of each packet can be extracted directly from the first path of each packet. However, in the case of concurrent packet reception, the peaks of each packet will be reflected on the same CIR. As Figure 4 shows, we notice a first peak at around 20 ns and a second peak 128 ns later (the delay is 128 ns in this case) at around 148 ns. Therefore, the first peak is detected as the first path index and the second peak will be detected by applying a matched filter on a window of 50 samples centered around the index of the first path + delay.

We can then extract the phase of arrival of the first packet as $PoA_{fp1} = arctan(\frac{Q_{fp1}}{I_{fp1}})$ and the phase of arrival of the second packet as $PoA_{fp2} = arctan(\frac{Q_{fp2}}{I_{fp2}})$ where $fp1$ is the index of the first path and $fp2$ is the index resulting from the matched filter detection.

### 3) Phase correction:

Phase extraction from CIR can present two main challenges. **CIR resolution:** Although the reception time on DW1000 has a time resolution of 15.6 ps, the CIR has only a resolution of 1 ns. Therefore, the first path position usually does not match exactly the index reported on the CIR. We tackle this issue by taking the average phase of the first path index $fp1$ and $fp1 + 1$. Similarly, for the second path, the result of the matched filter has more resolution than the CIR. In this case, we use a linear estimation of $fp2$ (basically a weighted average) to calculate the phase of the second path from two consecutive samples $s1$ and $s2$ where $s1 < fp2 < s2$.

**Phase wraparound:** The phase is represented between $-\pi$ and $\pi$. This means that if the phase increases beyond $\pi$ for instance, it will wraparound to $-\pi$. Since we are considering averages between consecutive samples, if one of the samples wrapped around, the resulting average becomes invalid. In this case, we map the sample that wrapped around between $-2\pi$ and $2\pi$ and we recalculate the average to end up with a correct phase.

### 4) AoA estimation and path correction:

Once we estimate the first and second peak phases, we compute the phase difference and calibrate it by adding a phase difference offset. The offset is calculated based on ground truth data. The purpose of the offset is to ensure that the measured phase difference values are always between $-\pi$ and $\pi$. Then we compute the path difference p similarly to the case of dual-antenna AoA estimation. With different types of UWB systems, the form factor of the antennas on the system may impact the accuracy of path difference measurements. The asymmetry between the transmitting antennas can result in incorrect path difference measurements. To correct the measurements, we build a path difference fitting polynomial based on measurements at multiple angles. Once we calculate our corrected path difference, we calculate AoA by using the same formula as baseline method to convert path difference to angle.

## IV. EVALUATION

### A. Experimental setup

In our experiments, we used DWM1002 (Fig. 3) as our anchor node and dual-antenna tag (Baseline AoA), and TREK1000 [19] as our single-antenna tag. We conducted the experiments in a room of size 4 m × 3 m in a residential building. We placed all the nodes on tripods at a height of 1.5 m height. We used frequency channel 7, with a preamble length of 128, and a data rate of 6.8 Mbps, which are typical settings used in similar concurrency-based studies in the literature. To compare between different anchors, we considered the use of 5 DWM1002 platforms.

### B. Feasibility of single-antenna AoA

In this section, we first compare the performance of AoA estimation single-antenna UWB radio (SA-AoA) compared to classical AoA estimation systems (baseline dual-antenna). Then, we study the feasibility of our system with different parameters.

*1) Comparison of single-antenna AoA with baseline dual-antenna AoA:*

In this section we compare the estimation of AoA between SA-AoA and the baseline AoA estimation provided by Decawave DWM1002. The baseline system combines AoA estimation using dual-antenna UWB devices and TWR to find the location of the target. In this experiment, we place the nodes at close proximity to have better control on ground truth angles and at a height of 35 cm. We collect angle measurements for multiple angles for both SA-AoA and the baseline system.

In the case of SA-AoA, we consider a delay of 128 ns. Results from Figure 5 show that for both SA-AoA and the baseline system, the average error is $3.81°$ with $4.17°$ of standard deviation for the baseline system and $2.61°$ of standard deviation for SA-AoA. This result shows that our system achieves a similar performance with one antenna at the tag compared to the performance of the baseline AoA estimation system by Decawave which has two antennas at the anchor thus improving cost and design efficiency.
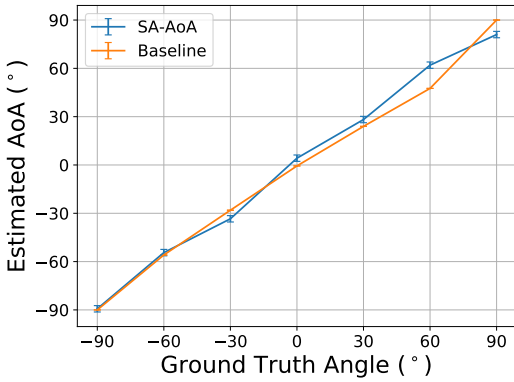


**Fig. 5:** Comparison between SA-AoA and baseline AoA estimation at different angles. The performance of AoA estimation is comparable between both systems

*2) Single-antenna AoA with different angles and delays:*

In the context of AoA-based localization, it is important to be able to estimate the angle-of arrival at any position in the localization space. For that purpose, we consider in our experiments a set of angles $(-90°, -60°, -30°, 0°, 30°, 60°, 90°)$ that covers most of the angle range.

We also want to investigate the usage of different delays between packet transmissions as different delays can be used in as a basis of different mac protocols.

We first consider the case of sending packets with large delays to receive two consecutive packets at the receiver tag (non-concurrent). We fix the delay to 600 $\mu s$ and we collect around 8000 angle measurements. Figure 6 shows the result of AoA estimation with single-antenna tag when using separately received packets. Due to the phase drift of the transmitters

and receiver, we cannot estimate the AoA correctly for non-concurrent packets, which implies the importance of concurrent transmissions.
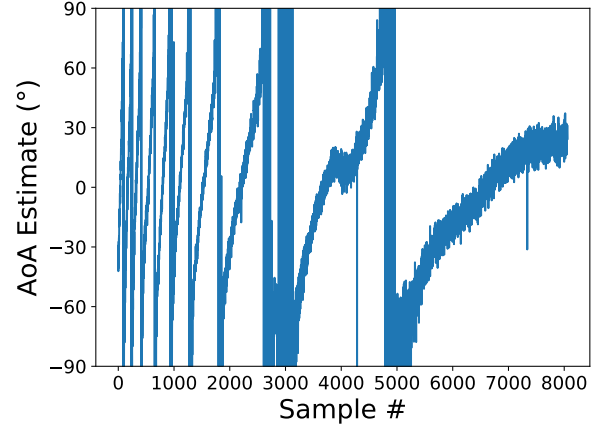


**Fig. 6:** Result of AoA estimation for non-concurrent packets. AoA estimate largely varies over time due to phase drift between received packets.

Next, we consider the small delays for AoA estimation (intra-anchor concurrency). In this scenario, we face the same problem of phase wraparound as presented in previous observations. As we test on a specific dual-antenna device, we define a generic phase difference offset for all delays although it can be fine-tuned for each delay separately. However, we still need to build a correction polynomial for each delay. Figure 7 shows the means and standard deviations of AoA estimation for a single-antenna tag when using different delays from 24 ns to 512 ns. We do not observe a large variation when using different delays because the phase drift is negligible in a short period of time. We only report a mean standard deviation of $0.96°$ among all delays. The receiver could not receive any packets beyond 512 ns since the receiver chip cannot identify which path comes first. Compared with the ground truth angle, the minimum mean error is only $0.56°$ in $-90°$ and the maximum mean error is $7.44°$ in $90°$.

*3) Single-antenna AoA at different distances:*

We also investigate the impact of distance on AoA estimation. We collect data at multiple angles at different distances with a delay of 128 ns. We consider two distances of 1 m and 2 m as allowed by our experiment space. As shown by Figure 8, SA-AoA performs well under different distances with mean errors of $5°$ and standard deviation of $4.20°$ for 1 m and mean errors of $5.6°$ and standard deviation of $4°$ for 2 m. This shows that for an indoor environment with limited space, our solution is largely insensitive to distance as opposed to time-based methods where ranging errors increase as a function of the distance [20].

*4) Single-antenna AoA on different devices:*

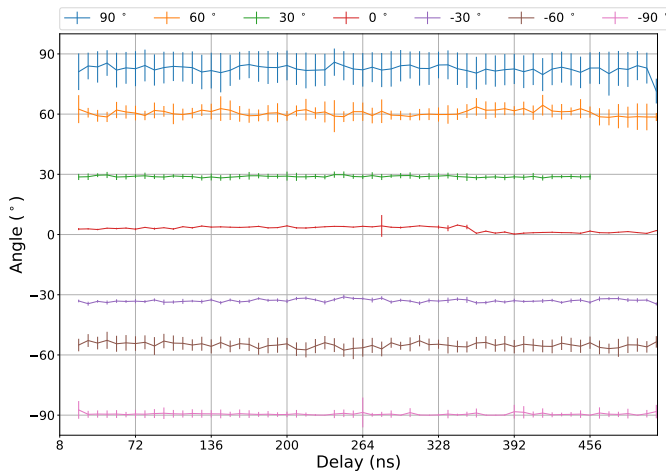Asymmetry in the design and manufacturing of dual-

**Fig. 7:** Single-antenna AoA estimation with different transmission delays (intra-anchor concurrency). No significant variation is observed.
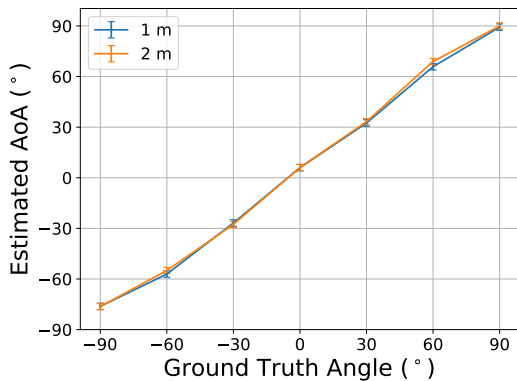


**Fig. 8:** Evaluation of SA-AoA with multiple distances and angles. The distance has negligible impact on the AoA estimation

around $0°$ for most ground truth angles and devices but can reach up to $9°$ in some cases.
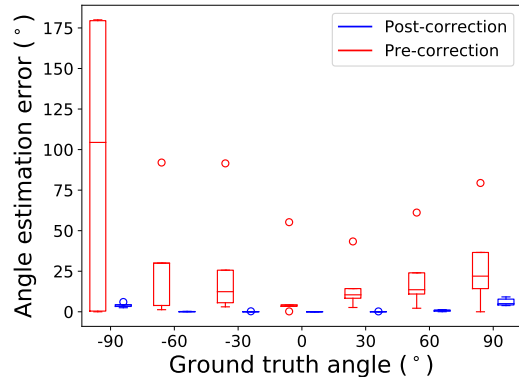


**Fig. 9:** Comparison of AoA estimation errors pre and post-correction for multiple angles on different dual-antenna UWB devices. Large IQRs in pre-corrected estimation errors are indicators of the asymmetry problem.

We can assume that the problem of asymmetry is generic in all dual-antenna UWB devices. This shows the benefit of using SA-AoA as this correction needs to be done only for anchors. While for other systems that rely on dual-antenna UWB devices as tags, the overhead of calibrating all tags is larger since typically in a localization system, the number of tags exceeds largely the number of anchors.

## V. DISCUSSION

The proposed technique is a receiver-side technology, in the sense that the receiver does not need to transmit packets. Thus, this approach can scale to unlimited number of devices just like GPS and some UWB-based techniques that have been proposed in the literature. As a result of our work, we have shown that it is possible to estimate AoA with such attractive scaling property.

AoA systems typically suffer from front-back ambiguity problem and unknown device orientation. The proposed approach can avoid the problem in most scenarios where we have some geometric constraints. Since we only have dual-antenna at anchors, we can assume known orientation of anchors and only send packets to devices inside the room from the front of the antenna. Hence, the transmitter antenna can be designed to transmit from only one side. The single-antenna tag then does not impose any limitation on front-back ambiguity and unknown orientation.

As mentioned in section IV, using different delays requires building a correction model for each delay. This can add some overhead to the initialization step of this system. However, we can argue that this overhead is minimal as the number of delays that can be used by the same system is limited and does not cover the full spectrum of delays that we evaluated.

antenna UWB devices can be the source of errors in AoA estimation systems. We measured angles on multiple devices of the same type (DWM1002) with a transmission delay of 128 ns for different angles. Each box plot in Figure 9 represents the combined mean angle estimation errors of different devices. We notice that the error box plots before correction have a large IQR (interquartile range). This shows that different devices can present a large difference in angle estimation under the same configuration (ground truth angle, delay). It is also noticeable that some devices exhibit drastic errors reaching around $180°$ of error for the angle $-90°$. These errors are the result of the phase wraparound problem. To mitigate this problem, we add a phase difference offset specific to each device to bound the phase difference measurements between $-\pi$ and $\pi$. Then, we build a $4^{th}$ order polynomial for each device to correct the path difference. From the post-correction box plots, we conclude that our correction is effective since the AoA estimation mean error is

In this work, we evaluated the proposed system by putting all the nodes at the same height to maximize the signal reception. We considered optimal conditions since the purpose of this work is to prove the feasibility of single-anchor AoA estimation. Although the signal reception can be reduced at different heights, we noticed that it doesn't impact considerably the AoA estimation.

## VI. Conclusions

In this paper, we introduced a novel approach to Angle-of-Arrival estimation using a single antenna at the receiver tags and dual antenna at the anchors. This configuration allows a good tradeoff for low-complexity and low-cost at the anchors, which are expected to be deployed in large numbers. The main idea behind the technique is the transmitters sending multiple packets concurrently and the tags receiving the concurrent packets simultaneously and extracting the phase information using CIR. We implemented and evaluated the system on Decawave hardware platform and found that the results with single-antenna AoA is similar to the dual-antenna approach.

## References

[1] M. Heydariaan, H. Dabirian, and O. Gnawali, "Angu-loc: Concurrent angle of arrival estimation for indoor localization with uwb radios," in *2020 16th International Conference on Distributed Computing in Sensor Systems (DCOSS)*. IEEE, 2020.

[2] *Beta PDoA kit User Manual*, Decawave, 2018.

[3] H. Mohammadmoradi, M. Heydariaan, and O. Gnawali, "Srac: Simultaneous ranging and communication in uwb networks," in *2019 15th International Conference on Distributed Computing in Sensor Systems (DCOSS)*. IEEE, 2019, pp. 9–16.

[4] D. K. Rout and S. Das, "Multiple narrowband interference mitigation using hybrid hermite pulses for body surface to external communications in uwb body area networks," *Wireless Networks*, vol. 23, no. 2, pp. 387–402, 2017.

[5] H. Mohammadmoradi and O. Gnawali, "Study and mitigation of non-cooperative uwb interference on ranging," in *EWSN*, 2019, pp. 142–153.

[6] F. Ferrari, M. Zimmerling, L. Thiele, and O. Saukh, "Efficient network flooding and time synchronization with glossy," in *Proceedings of the 10th ACM/IEEE International Conference on Information Processing in Sensor Networks*, 2011, pp. 73–84.

[7] M. Doddavenkatappa, M. C. Chan, and B. Leong, "Splash: Fast data dissemination with constructive interference in wireless sensor networks," in *10th USENIX Symposium on Networked Systems Design and Implementation (NSDI 13)*. Lombard, IL: USENIX Association, Apr. 2013, pp. 269–282. [Online]. Available: https://www.usenix.org/conference/nsdi13/technical-sessions/presentation/doddavenkatappa

[8] B. Kempke, P. Pannuto, and P. Dutta, "Surepoint: Exploiting ultra wideband flooding and diversity to provide robust, scalable, high-fidelity indoor localization: Demo abstract," in *Proceedings of the 14th ACM Conference on Embedded Network Sensor Systems CD-ROM*, ser. SenSys '16. New York, NY, USA: Association for Computing Machinery, 2016, p. 318–319. [Online]. Available: https://doi.org/10.1145/2994551.2996541

[9] D. Lobba, M. Trobinger, D. Vecchia, T. Istomin, and G. P. Picco, "Concurrent transmissions for multi-hop communication on ultra-wideband radios." in *EWSN*, 2020, pp. 132–143.

[10] P. Corbalán and G. P. Picco, "Concurrent ranging in ultra-wideband radios: Experimental evidence, challenges, and opportunities," in *Proceedings of the 2018 International Conference on Embedded Wireless Systems and Networks*, ser. EWSN '18. USA: Junction Publishing, 2018, p. 55–66.

[11] P. Corbalán, G. P. Picco, and S. Palipana, "Chorus: Uwb concurrent transmissions for gps-like passive localization of countless targets," in *2019 18th ACM/IEEE International Conference on Information Processing in Sensor Networks (IPSN)*, 2019, pp. 133–144.

[12] B. Growindhager, M. Stocker, M. Rath, C. A. Boano, and K. Römer, "Snaploc: An ultra-fast uwb-based indoor localization system for an unlimited number of tags," in *2019 18th ACM/IEEE International Conference on Information Processing in Sensor Networks (IPSN)*, 2019, pp. 61–72.

[13] B. Großwindhager, C. A. Boano, M. Rath, and K. Römer, "Concurrent ranging with ultra-wideband radios: From experimental evidence to a practical solution," in *2018 IEEE 38th International Conference on Distributed Computing Systems (ICDCS)*, 2018, pp. 1460–1467.

[14] M. Heydariaan, H. Mohammadmoradi, and O. Gnawali, "R3: Reflection resilient concurrent ranging with ultra-wideband radios," in *2019 15th International Conference on Distributed Computing in Sensor Systems (DCOSS)*. IEEE, 2019, pp. 1–8.

[15] T. Wang, H. Zhao, and Y. Shen, "An efficient single-anchor localization method using ultra-wide bandwidth systems," *Applied Sciences*, vol. 10, no. 1, p. 57, 2020.

[16] M. McLaughlin, G. MARROWI, and I. Dotlic, "Method and apparatus for determining location using phase difference of arrival," Dec. 17 2019, uS Patent App. 15/974,412.

[17] M. McLaughlin, J. Niewczas, I. Dotlic, and B. Verso, "Method and apparatus for determining the angle of departure," Aug. 6 2020, uS Patent App. 16/780,004.

[18] M. McLaughlin, D. Neirynck, and C. McElroy, "Timing recovery for use in an ultra-wideband communication system," May 17 2018, uS Patent App. 15/868,026.

[19] *TREK1000 User Manual*, Decawave, 2018.

[20] N. Smaoui, O. Gnawali, and K. Kim, "Study and mitigation of platform related uwb ranging errors," in *2020 International Conference on COMmunication Systems NETworkS (COMSNETS)*, 2020, pp. 346–353.